Vaccine 37 (2019) 4561–4567

Contents lists available at ScienceDirect

Vaccine

journal homepage: www.elsevier.com/locate/vaccine

Statistical projection of post-vaccination antibody kinetics between dosing schedules

Anthony Almudevar [a,*], Ravinder Kaur [b], Michael Pichichero [b]

[a] Department of Biostatistics and Computational Biology, University of Rochester, Rochester, NY, United States
[b] Center for Infectious Diseases and Immunology, Rochester General Hospital Research Institute, Rochester, NY, United States

ARTICLE INFO

Article history:
Received 6 June 2018
Received in revised form 1 May 2019
Accepted 10 June 2019
Available online 28 June 2019

Keywords:
Vaccines doses
Kinetics
Modeling

ABSTRACT

Determining a recommended dosage schedule is a crucial component of vaccine administration, and is often subject to reassessment. Ideally, recommendations will be supported by multiple arm clinical trials. However, the considerable cost in both resources and time means that a method of predicting post-vaccine humoral antibody levels associated with a hypothetical schedule using data collected from a currently implemented schedule would be of significant benefit to vaccination practice.

In this paper we propose such a methodology, which permits statistical estimation of the population mean and standard deviation of log transformed antibody titers of various post-vaccination time points of a hypothetical schedule, using a longitudinal sample of antibody titers from an observed schedule. The method is based on the decomposition of humoral antibody kinetic history into distinct phases, for example, peak phase, decay phase and post-booster phase. The method is feasible because each phase has its own discernable kinetic laws. Of particular interest will be estimation of antibody levels immediately preceding a booster dose (typically the lowest level attained during the schedule), and the antibody levels following a booster dose.

1. Introduction

Vaccine efficacy is known to be highly dependent on dosage schedule (which defines collectively the number of doses, age administered, time interval between doses, and inclusion/exclusion of booster). For many vaccines the minimum number of doses required for protection is not known, and the problem is further complicated by sensitivity to the dosage time points.

For example, the recommended dosage schedule for the pneumococcal conjugate vaccine PCV13 has recently become an important public health question. In 2010, PCV13 was licensed in the US for a 3 + 1 schedule.. Primary doses are given at 2, 4, 6 months of age, and the booster at 12–15 months. On the other hand, different PCV13 schedules are recommended across Europe and other countries, after consideration of the epidemiology, disease burden, immunogenicity of the vaccine, its compatibility with other vaccines and cost to purchase. Especially with consideration to cost and a focus on invasive diseases (IPD), the World Health Organization (WHO) recently updated their PCV policy to support use of 3 doses as either 3 + 0 or 2 + 1 schedules [28,3]. Most European countries have adopted the 2 + 1 schedule according to their routine infant immunization schedule. With consideration of the escalating costs to provide current and anticipated future vaccination coverage for additional vaccines as a national public health policy, the U.S.Centers for Disease Control Advisory Committee on Immunization Practices (CDC-ACIP) has convened a working group to evaluate transition from a 3 + 1 to a 2 + 1 schedule for PCV administration to infants and children. The decision to reduce the number of doses of PCV13 (and its precursors) is informed by multiple arm clinical trials, which generally report that while reduction of aggregate dosage reduces humoral antibody concentrations, the various dosage schedules considered generally maintain minimum protective levels [10,25,13,9].

In general, reevaluation of vaccine dosage schedules occurs on a regular basis, as an inevitable component of vaccine administration. Recent examples include human rabies [18], HPV [17] and measles, mumps, and rubella (MMR) [14]. Ideally, dosage schedule change recommendations would be supported by multiple arm clinical trials. However, the considerable cost in both resources and time means that a method of predicting post-vaccine humoral antibody levels associated with a hypothetical schedule using data collected from a currently implemented schedule would be of significant benefit to vaccination practice.

* Corresponding author at: University of Rochester, Dept of Biostatistics and Computational Biology, 265 Crittenden Boulevard, CU 420630, Rochester, NY 14642-0630, United States.
E-mail address: Anthony_Almudevar@urmc.rochester.edu (A. Almudevar).

https://doi.org/10.1016/j.vaccine.2019.06.017
0264-410X/

In this paper we propose such a methodology, which permits statistical estimation of the population mean and standard deviation of log transformed antibody titers of various post-vaccination time points of a hypothetical schedule, using a longitudinal sample of antibody titers from an observed schedule. The method is based on the decomposition of humoral antibody kinetic history into distinct phases: peak phase, decay phase and post-booster phase. The method is feasible because each phase has its own discernible kinetic laws. Of particular interest will be estimation of antibody levels immediately preceding a booster dose (typically the lowest level attained during the schedule), and the antibody levels following a booster dose.

2. Methods

The method is demonstrated using six routine vaccines administered to children. Details of the study design have been described previously [7,12]. All children received age-appropriate vaccinations with products approved by the US Food and Drug Administration. The analysis is based on 1538 post-vaccination antibody titers collected from 549 children. The vaccines studied were diphtheria toxoid (DT); acellular pertussis and polyribosylribitol phosphate (PRP)-tetanus toxoid (TT) conjugate vaccines; pertussis toxoid (PT); pertactin (PRN); and filamentous hemagglutinin (FHA) (Sanofi Pasteur or GlaxoSmithKline; brand name for these vaccines were Pentacel or Pediarix). Primary doses were administered at approximately 2, 4, 6 months of age, with a booster targeted at 15–18 months (most boosters we administered at the 18 months visit, but ranged from 15 to 24 months). The primary dose of pneumococcal conjugate vaccine Prevnar 7 or 13 (Pfizer) was also given concurrently to all enrolled children at 2, 4, 6 months of age and the booster dose at the 12 m or 15 m visit (in an approximate ratio of 20:80). Since Prevnar vaccines are conjugated to the Crm197 carrier protein, which is a modified diphtheria toxoid, children can have an additional antibody response contribution to DT because of this Crm197 component [24,2,27,5].

Blood samples were obtained at prospective visits at child age 6,9,12, 15, 18, 24 36, 48 and 72 months Immunoglobulin G antibody levels to DT, TT, PT, FHA, PRN, and PRP were measured from plasma samples by enzyme-linked immunosorbent assays, as described in [21,20].The minimum protective antibody level (MPL) for DT and TT when measured with enzyme-linked immunosorbent assay is 0.1 IU/mL; for Haemophilus influenza type B polysaccharide, (PRP) concentration is 0.15 μg/mL [22,23]. Correlates of protection for Pertussis antigens have not been established; however, a titer of 8 ELISA units (ELU)/mL has been proposed for PT, PRN and FHA [26].

2.1. Structure of data

The data can be organized as 4-tuples (y_i, t_i, s_i, v_i), $i = 1, \cdots, n_T$, where y_i is the ith $\log_2$-transformed antibody response, collected from subject s_i at age t_i months and visit v_i. The visit label v_i represents a schedule of regular visits where blood samples were taken. The visits are labeled 6 m, 9 m, 12 m, 15 m, 18 m, 2y, 3y, 4y, 5y. The 3rd vaccine dose of the 3 + 1 schedule is given at visit $v_i = 6$ m, and the booster at visit $v_i = 15$ m, 18 m or 2y for most subjects. The actual age is generally higher than that indicated by the visit label, and may differ considerably for later visits 4y and 5y.

2.2. Decay model

Post-vaccination decay kinetics was been widely described in the literature. We use the antibody decay model proposed in [11] (see also [8,15]). Decay, following vaccination, has been widely observed to follow the equation

$$y_t = y_{t_0}\left(\frac{t - t_v}{t_0 - t_v}\right)^k, \quad t > t_0 > t_v, \tag{1}$$

t = subject age,
t_v = age at vaccination (finaldose),
t_0 = age at peak antibody level,
y_t = antibody level at age t,
k = decay parameter.

The model is tractable, and can be fit using linear regression models following the log-log transformation:

$$\log_2 y_t = \log_2 y_{t_0} + k[\log_2(t - t_v) - \log_2(t_0 - t_v)] \tag{2}$$

The validity of Eq. (1) is further discussed in [1], in the form of a literature review, and the development of a cellular-level first principles model which predicts specifically $k \approx -1$, although this may be only one component of humoral immunity (see also, for example, [6]).

2.3. Projection by kinetic history decomposition

We modeled the data using observed and projected dose schedules, $S = 2/4/6 + 18$ and Schedule 2 $(S^*) = 2/4 + 12$ (we set the time of booster $(t_b) = 18$ for schedule S for notational convenience, but the model allows varying booster ages). We let X_t, X_t^* be the mean $\log_2$ antibody levels at time t following schedules S ,and alternative dose schedule S* respectively. The objective was to estimate antibody levels $X_{t'}^*$ for selected values of time t' based on data observed from the original dose schedule S.

We will developed estimators specifically for antibody response at 12 months X_{12}^* and following booster vaccination $X_{t_p}^*$, for some time $t_p > t_b$. The quantity X_{12}^* was the antibody level immediately prior to the booster in schedule S^*, and is therefore likely to represent the lowest antibody level in the kinetic history, thus $X_{t_p}^*$ represents a post-booster antibody level.

We decomposed kinetic history into three phases, which are listed in Table 1 with their respective age ranges. In principle, any antibody level along the original schedule X_t or the alternate schedule X_t^* can be decomposed into components associated with a single kinetic history phase. We show how this permits projection between schedules even when the time points and lengths between phases differ. See supplement 2 for equations and details.

2.4. Statistical models

The problem of modeling and estimating post-vaccination antibody decay has been widely discussed in the literature [1,19]. Modifications of the power-law model described in Section 2.2 [11] as well as nonparametric alternatives have been proposed in [6], [4] and [18]. We will show that the power-law decay model is suitable for this application, but in general this must be verified.

Table 1
Phases of post-vaccination antibody kinetics. Age range in months is given for observed and projected schedules $S = 2/4/6 + 18$ and $S^* = 2/4 + 12$.

Phase	S	S^*
1 - Final primary dose to post-peak decay phase	6–8	4–6
2 - Decay phase up to booster	8–18	6–12
3 - Booster and post-booster phase	≥ 18	≥ 12

Antibody decay models often rely on repeated subject measures, so statistical models must correctly model this structure. In general, the two most common methods for analyzing longitudinal data are mixed effects models (per-subject analysis) and GEE methods (population level analysis) [16]. The latter accounts for repeated measure structure by explicitly modeling the subject-level correlation that this structure induces in the responses. While [6], [4] and [18] use mixed effects models, we used the GEE method for this application for a number of reasons. The GEE method yields unbiased population estimates, which is the correct emphasis when estimating, for example, percentage of subjects above MPL at a fixed time point. In addition, the GEE method employs analytical methods which are particularly convenient when developing compound estimators based on separate GEE models. See supplement 2 for more detail.

The code and data used to calculate Figs. 1–3 and Tables 3, S.1–S.7 are included in supplement 3 A glossary of the notation is given in Table S.8

3. Results

A critical assumption underlying the estimation of antibody decay after the booster dose is that the increase in log_2 antibody levels induced by the booster does not depend on the initial value, and so is the same for 2/4/6 + 18 month schedule and 2/4 + 12 schedules. To test this assumption we used Table 2 from Goldblatt et al. [10] where serotype-specific pneumococcal IgG concentrations μg/mL in child subjects following both vaccine schedules were reported. In Table 2 our model is used to predict results reported by Goldblatt et al. [10]. The final two columns give the predicted respective increases on a log_2 scale based on our model. The mean difference in increase between the groups within serotype is −0.038 (SE = 0.127), considerably smaller than the apparent variation across serotypes, and not significantly different from zero. This result conforms to the critical assumption.

3.1. Phase components

Fig. 1 shows the mean log_2 antibody response curve for each of the 6 vaccines for the S = 2/4/6 + 18 schedule fit over the entire study range. The MPL is superimposed (gray line) on the plots. Table S.1 gives the estimates of correlation and standard deviation $\hat{\rho}, \hat{\sigma}$ as well as sample sizes.

Data for visit range 6 m to 15 m was used to model the post primary dose decay phase of antibody levels up to the booster. Fig. 2 plots the resulting fitted models on a double-logarithmic scale. The apparent linearity of the plots conform well to the measured data.

Data for visit range 15 m−5 y was used to model post-booster antibody levels. The analysis used booster age as a baseline. Since this varies by subject, the time scale used was age since booster.

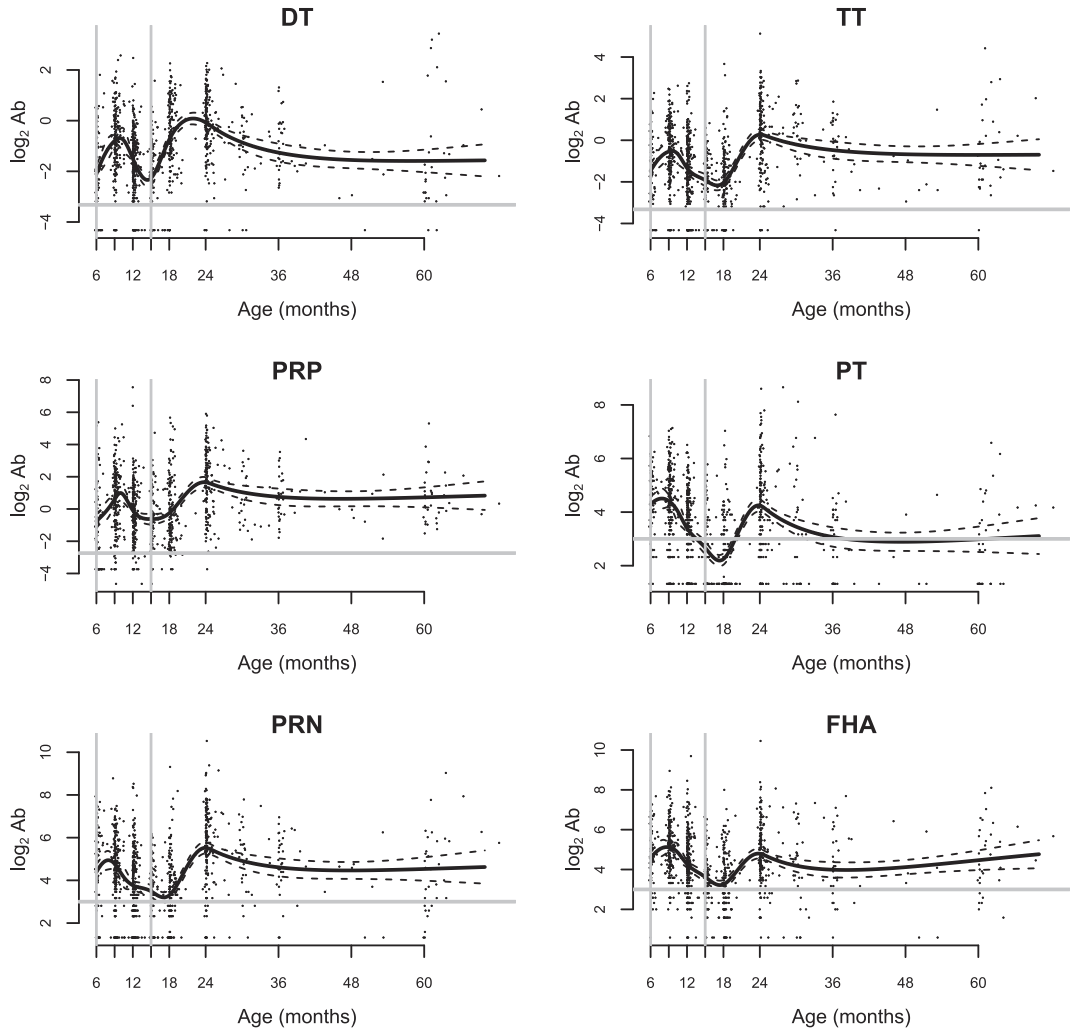

Fig. 1. Piecewise linear spline estimate of $\log_2$ Ab levels. Black line gives ND filtered estimate. Vertical gray lines indicate third vaccine dose at visit 6 m and boosters at visit 15 m or later. Horizontal gray line shows MPL.

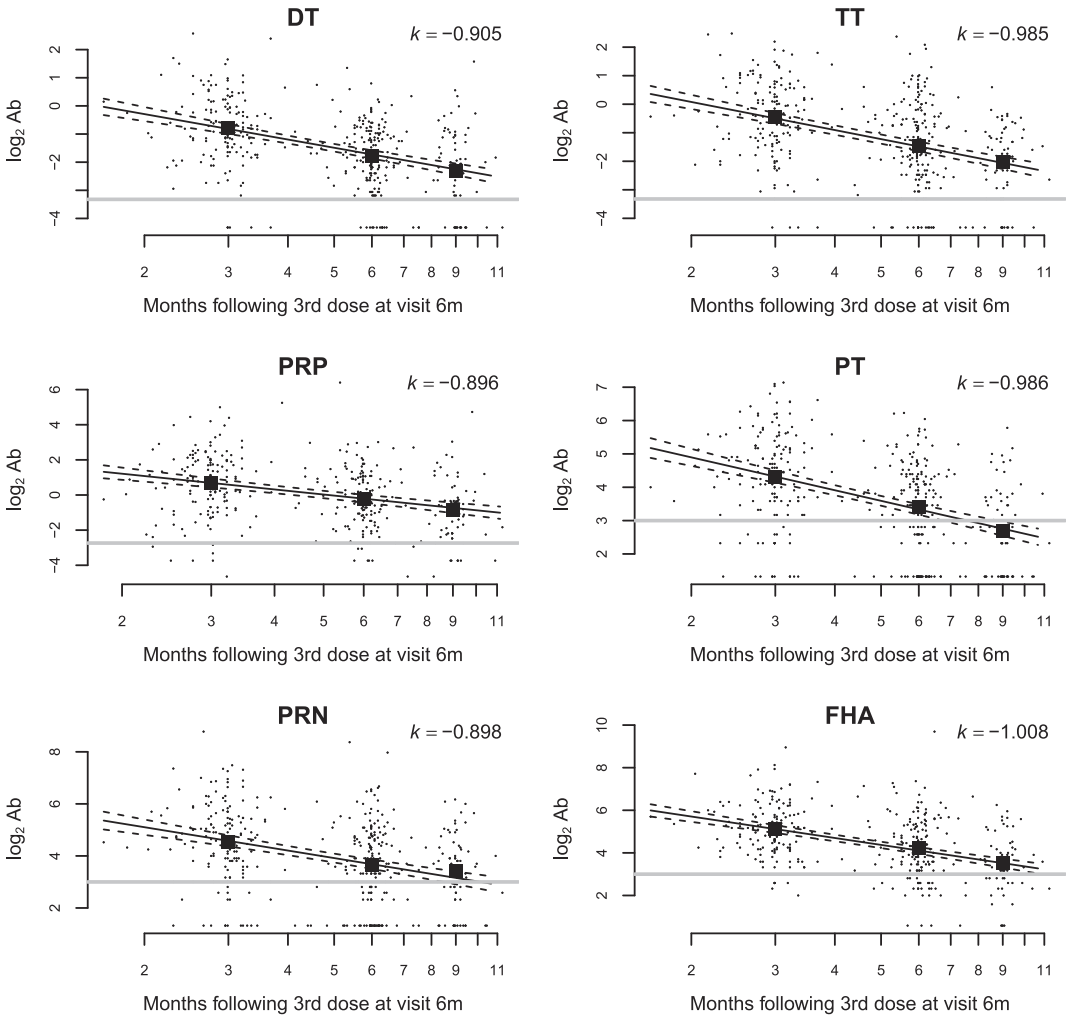

Fig. 2. Linear decay model on doubly log-transformed data, using visits 9 m −15 m. Horizontal axis represents time since third vaccine dose of schedule*S*. Marginal 95% confidence bounds are indicated by the dashed lines. The sample mean for each visit 9 m, 12 m, 15 m are superimposed (■).

Fig. 3 shows the resulting fits. For most antibodies, the shapes are as expected, showing a relatively rapid increase in antibody level, followed by slower decay. The clear exception is the DT antibody, since at the baseline time children have already received a Prevnar 7 or 13 booster which will stimulate a DT response. Thus, children essentially receive two DT boosters, and the projection model used for this demonstration therefore does not apply, in particular, the decay interval following the booster Δ_2 is not interpretable for DT. This is evident in Fig. 3, in which it can be seen that the rise in antibody level 6 months after the booster is clearly smaller for DT than for the remaining antibodies.

Table 3 shows the estimated percentage of subjects above the minimum protective level of antibody for each of the vaccines 21 months following a booster for schedules S, S^*, respectively). For schedule S, antibody levels are predicted to exceed MPL for at least 99% of children for antibodies TT and PRP. On the other hand, for schedule S^*, only 91.5% and 89.7% of children are predicted to exceed MPL for these antibodies.

Over the entire study range of vaccines and age of children, the model predicts the antibody levels with high accuracy for schedule 2/4/6±18, while noting the variable booster age (Fig. 1). If all boosters were administered at visit 18 m, the decay phase would extend to this visit, with the booster effect not evident until the subsequent visit 2y. On the other hand, because a proportion of children received the booster at the 15 m visit (approximately 18% for PRP; 7% for the remaining vaccines) the booster effect is evident as a mixture, with some degree of booster effect visible at visit 18 m. This is most apparent for PRP, consistent with a higher proportion of children given this booster at the 15 m visit.

The DT antibody represents an interesting special case. Most children in this study were given a Prevnar 7 or 13 vaccine at the 15 m visit, which stimulates a DT antibody response. Accordingly, the DT antibody levels of Fig. 1 decay until visit 15 m, following which a strong booster effect is evident at visit 18 m.

Details of the estimation of the post primary dose to post peak decay phase, the decay phase up to the booster and the booster to post booster phase are shown, respectively, in Tables S.2, S.3, and S.4. Each table gives, for each antibody, the relevant estimate and standard error, sample sizes used in the fit, and an estimation of response standard deviation Table S.4 gives estimates and standard errors for the decay interval following the booster Δ_2.Table S.5 gives estimates and standard errors for antibody levels following the booster for the observed schedule S.

3.2. Population parameters $\widehat{\rho}, \widehat{\sigma}$.

For each antibody the analyses yields 4 estimates of standard deviation, based on the entire visit range (Table S.1), then the 3

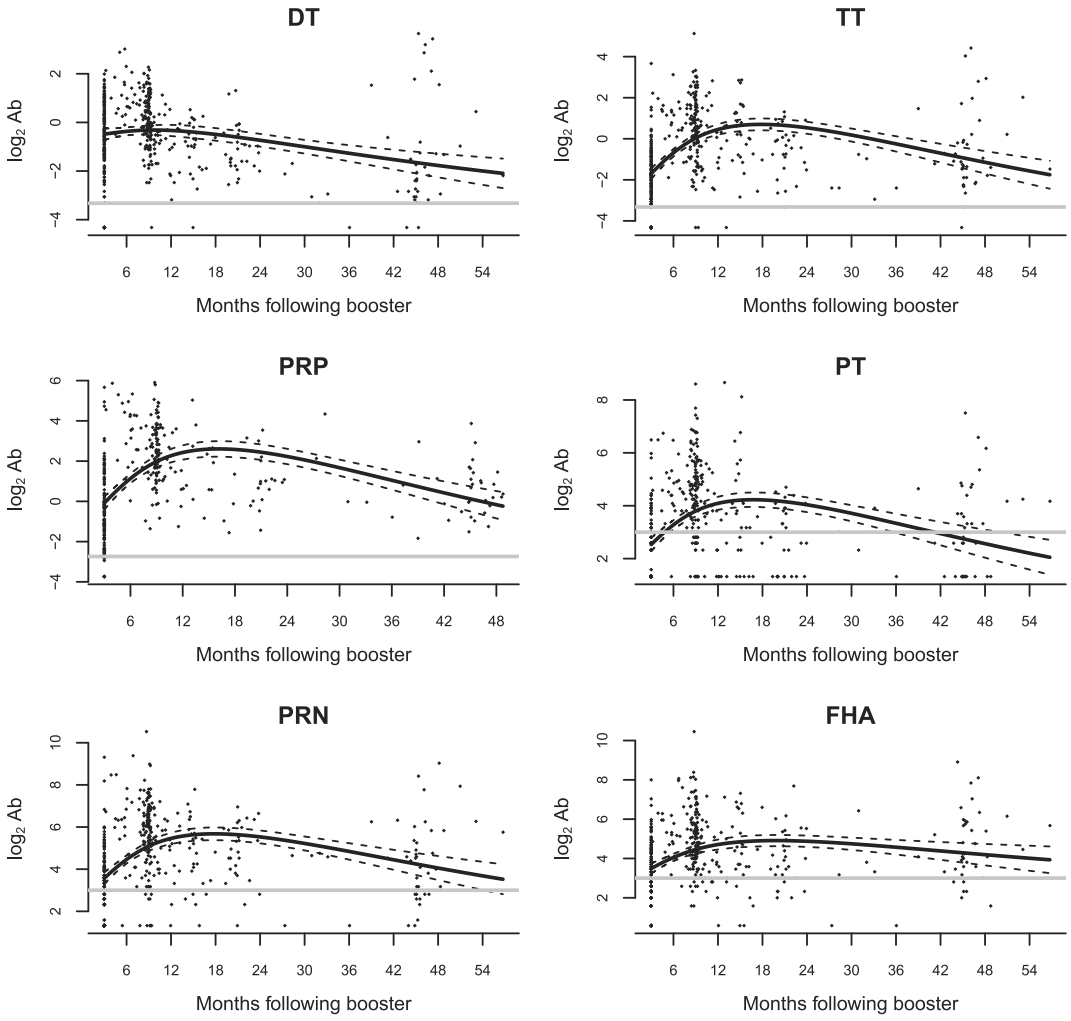

Fig. 3. Spline fit for post-booster $\log_2$ Ab levels. Marginal 95% confidence bounds are indicated by the dashed lines. Horizontal gray line shows MPL.

Table 2
Serotype-specific pneumococcal IgG concentrations (μg/mL) in child subjects following both 2 and 3 dose vaccine schedules (Data reproduced from Table 3 of Goldblatt et al. [10]); $\log_2$Ab increases for each dose group are appended.

	3 Dose		2 Dose		3 Dose	2 Dose
Serotype	Pre-	Post-	Pre-	Post-	Increase $\log_2$ Ab	Increase $\log_2$ Ab
1	0.68	1.48	0.57	10.84	4.08	4.25
4	0.4	12.95	0.27	9.48	5.02	5.13
5	1.31	9.15	0.75	6.796	2.8	3.18
6B	0.69	5.57	0.94	5.89	3.01	2.65
9V	0.43	7.01	0.3	6.2	4.03	4.37
14	1.64	20.92	0.91	12.62	3.67	3.79
18C	0.32	4.53	0.24	2.77	3.82	3.53
19F	1.16	14.74	1.47	10.78	3.67	2.87
23F	0.5	5.79	0.39	4.47	3.53	3.52

Table 3
Estimated percentage of protected subjects (above MPL) 21 months following booster. In this example, $t = 39$, 33 months for schedules S, $S*$, respectively. Minimum protective levels (MPL) are listed for reference.

Ab	MPL	X_{39}	% Protected	X^*_{33}	% Protected	σ
DT	−3.322		–	–	–	–
TT	−3.322	0.534	99.2	−1.105	91.5	1.614
PRP	−2.737	2.228	99.5	−0.335	89.7	1.903
PT	3.000	4.036	76.4	3.863	72.5	1.442
PRN	3.000	5.531	93.4	4.734	84.9	1.680
FHA	3.000	4.875	89.1	4.105	76.6	1.521

visit ranges 6 m, 9 m–15 m, 15 m–5 y (Tables S.2, S.3, S.4, respectively). The estimates are comparable between visit ranges, so we accept a single estimate based on the entire data set (Table S.1).

Similarly, for each antibody the analyses yields 3 estimates $\widehat{\rho}$, based on the entire visit range (Table S.1), then the 2 visit ranges 9 m–15 m, 15 m–5y (Tables S.3, S.4, respectively). These estimated pairwise correlation coefficients ρ in antibody levels tend to be highest for visit range 9 m–15 m ($\widehat{\rho} \in [0.888, 0.958]$), and lowest for visit range 15 m–5 y ($\widehat{\rho} \in [0.0, 0.354]$). That estimation of correlation coefficient ρ would be difficult for the 15 m–5 y range is expected. The mean difference in age for within-subject observations was approximately 20 months. Under the ARC correlation model, for observed correlation in mean antibody levels $\rho = 0.85$ (representative of Table S.1), the correlation between within-subject observations separated in age by 20 months would be $\rho^{20} \approx 0.039$. Thus, as for estimates of standard deviation$\widehat{\sigma}$, we accept a single estimate based on the entire data set (Table S.1).

3.3. Projection of post-vaccination antibody kinetics

We then use GEE modeling to calculate standard estimates of the projection estimates of antibody levels at 12 months and post-booster X^*_{12} and $X^*_{t_p}$ (post-booster estimates for DT are not given due to the effect on DT antibodies induced by the Prevnar 7 and 13 boosters). Accepting constant variability and mean autocorrelation σ^2 and ρ respectively Table S.6 summarizes estimates of the correlation between measured antibody levels at 6 months X_6 and decay interval Δ_1 ($\widehat{\rho}_{12}$); $\bar{X}_6$ and decay interval Δ_2 ($\widehat{\rho}_{13}$); and post-vaccination and post-booster decay intervals Δ_1 and Δ_2 ($\widehat{\rho}_{23}$). As might be expected, the correlation between 6-month levels and the post-booster decay interval $\widehat{\rho}_{13}$ is uniformly smallest, representing the largest separation in time between phases. It is also worth noting that the correlations are all negative which is to be expected. Consider two projection components representing adjacent kinetic phases. The respective contributions of those visits within each phase nearest to each other will be opposite in sign. Since this will be the dominant contribution to correlation, we can anticipate that the aggregate correlation will be negative. The estimated standard errors of the projections will therefore be smaller than the "naive" estimates, that is, those calculated assuming independence.

Table S.7 summarizes the projection estimates and their standard error. MPL antibody levels are also listed for reference. It can be seen that the lowest pre-booster antibody levels X^*_{12} are below MPL for all antibodies. In contrast, for schedule S only antibody PT was significantly below MPL immediately preceding the booster, with $X_{18} = 2.533 < 3.00 = MPL$ (Table S.5).

Also note that the mean post-booster $\log_2$ antibody levels $X^*_{t_p}$ for the projected schedule S^* are consistently above MPL at all post-booster times $t_p = 21, 33, 45$ consider in the analysis. As expected these values are also consistently below the corresponding antibody levels X_t for observed schedule S (Tables S.5, S.7).

4. Discussion

Here we have described a method of employing antibody kinetic data observed from one vaccine dosage schedule to estimate antibody concentrations for alternative projected schedule. The method was able to estimate standard errors for all estimates, and could estimate both population mean $\log_2$ antibody levels and quantiles (or percentage exceeding minimum protective levels (MPL)). The method was demonstrated using six commonly administered childhood vaccines. The impact of dosage reduction was precisely predicted, yielding both aggregate population antibody kinetics and estimates of reduction in protection.

The method depends on the decomposition of post-vaccination antibody kinetics into distinct phases, including peak antibody production, antibody decay phase, and post-booster phase. This allows the application of precise antibody kinetic laws for the purpose of projecting antibody levels between phases of differing times and lengths. The widely reported power-law decay model of Honorati et al. [11] was used. In addition, a simple booster effect model was proposed, which was shown to be consistent with data from multiple dosage trials reported by Goldblatt et al. [10].

As consistently reported [10,25,13,9], dosage reduction generally results in lower humoral antibody levels, the objective being to ensure that these levels remain well above MPL. For this reason, it is important to examine quantiles as well as population means. The percentage protected (above MPL) can be directly estimated assuming the $\log_2$ antibody response at time t is approximately normally distributed with mean X_t or X^*_t and standard deviation $\widehat{\sigma}$.

The data have a longitudinal structure that includes repeated measures from single subjects. Statistical models for analyzing this form of data generally fall into one of two categories [16]. Mixed effects models provide a subject-level analysis, allowing separate response curves for each subject which conforms to specific distributional properties. Generalized estimating equations (GEE), in contrast, model a single population level response curve. Repeated measure structure is accounted for by explicitly modeling the correlation which is induced in the responses, allowing for the efficient estimation of regression coefficients and the accurate estimation of standard error. Thus, we used GEE methods.

Further refinement is possible. Antibody decay models have received more attention in recent years [6,1]. In addition, study by Goldblatt et al. [10], it has been speculated that, counter intuitively, it is possible in at least some vaccines that post-booster antibody levels may be *negatively* correlated with pre-booster levels. However, any such refinements can likely be accommodated into the proposed statistical framework.

Declaration of Competing Interest

None.

Acknowledgement

This study was supported by NIH grant R03HD088909 (PI Ravinder Kaur). Matt Morris, PhD, provided useful advice in preparing the manuscript.

Funding

This study was funded by R03 HD088909-02 (PI: Kaur).

Appendix A. Supplementary material

Supplementary data to this article can be found online at https://doi.org/10.1016/j.vaccine.2019.06.017.

References

[1] Almudevar A. A model for the regulation of follicular dendritic cells predicts invariant reciprocal-time decay of post-vaccine antibody response. Immunol Cell Biol 2017;95(9):832–42.
[2] Bröker M. Potential protective immunogenicity of tetanus toxoid, diphtheria toxoid and cross reacting material 197 (crm197) when used as carrier proteins in glycoconjugates. Hum Vaccin Immunother 2016;12(3):664–7.
[3] Conklin M, Loo JD, Kirk J, Fleming-Dutra KE, Knoll MD, Park DE, et al. Systematic review of the effect of pneumococcal conjugate vaccine dosing

schedules on vaccine-type invasive pneumococcal disease among young children. Pediatr Infect Dis J 2014;33(Suppl):S109.
[4] David M-P, Van Herck K, Hardt K, Tibaldi F, Dubin G, Descamps D, et al. Long-term persistence of anti-HPV-16 and-18 antibodies induced by vaccination with the as04-adjuvanted cervical cancer vaccine: modeling of sustained antibody responses. Gynecol Oncol 2009;115(3):S1–6.
[5] Findlow H, Borrow R. Interactions of conjugate vaccines and co-administered vaccines. Hum Vaccin Immunothr 2016;12(1):226–30.
[6] Fraser C, Tomassini JE, Xi L, Golm G, Watson M, Giuliano AR, et al. Modeling the long-term antibody response of a human papillomavirus (HPV) virus-like particle (VLP) type 16 prophylactic vaccine. Vaccine 2007;25(21):4324–33.
[7] Friedel V, Zilora S, Bogaard D, Casey JR, Pichichero ME. Five-year prospective study of paediatric acute otitis media in rochester, ny: modelling analysis of the risk of pneumococcal colonization in the nasopharynx and infection. Epidemiol Infect 2014;142(10):2186–94.
[8] Gesemann M, Scheiermann N. Quantification of hepatitis b vaccine-induced antibodies as a predictor of anti-hbs persistence. Vaccine 1995;13(5):443–7.
[9] Goldblatt D, Southern J, Andrews NJ, Burbidge P, Partington J, Roalfe L, et al. Pneumococcal conjugate vaccine 13 delivered as one primary and one booster dose (1+ 1) compared with two primary doses and a booster (2+ 1) in uk infants: a multicentre, parallel group randomised controlled trial. Lancet Infect Dis 2018;18(2):171–9.
[10] Goldblatt D, Southern J, Ashton L, Richmond P, Burbidge P, Tasevska J, et al. Immunogenicity and boosting after a reduced number of doses of a pneumococcal conjugate vaccine in infants and toddlers. Pediatr Infect Dis J 2006;25(4):312–9.
[11] Honorati MC, Palareti A, Dolzani P, Busachi CA, Rizzoli R, Facchini A. A mathematical model predicting anti-hepatitis b virus surface antigen (hbs) decay after vaccination against hepatitis b. Clin Exp Immunol 1999;116 (1):121–6.
[12] Kaur R, Morris M, Pichichero ME. Epidemiology of acute otitis media in the postpneumococcal conjugate vaccine era. Pediatrics 2017;140(3):e20170101.
[13] Kent A, Ladhani SN, Andrews NJ, Scorrer T, Pollard AJ, Clarke P, et al. Schedules for pneumococcal vaccination of preterm infants: An RCT. Pediatrics 2016;138 (3):e20153945.
[14] Kim D, Riley LE, Hunter P. Advisory committee on immunization practices recommended immunization schedule for adults aged 19 years or older - United States, 2018. MMWR Morb Mortal Wkly Rep 2018;67(5):158.
[15] López EL, Contrini MM, Mistchenko A, Kieffer A, Baggaley R, Di Tanna GL, et al. Modeling the long-term persistence of hepatitis a antibody after a two-dose vaccination schedule in argentinean children. Pediatr Infect Dis J 2015;34 (4):417–25.
[16] McCulloch CE, Searle SR, Neuhaus JM. Generalized linear, and mixed models. 2nd. New Jersey: John Wiley & Sons; 2008.
[17] Meites E. Use of a 2-dose schedule for human papillomavirus vaccination - updated recommendations of the advisory committee on immunization practices. MMWR Morb Mortal Wkly Rep 2016;65.
[18] Mittal MK. Revised 4-dose vaccine schedule as part of postexposure prophylaxis to prevent human rabies. Pediatr Emerg Care 2013;29 (10):1119–21.
[19] Naud PS, Roteli-Martins CM, DeCarvalho NS, Teixeira JC, deBorba PC, Sanchez N, et al. Sustained efficacy, immunogenicity, and safety of the hpv-16/18 as04-adjuvanted vaccine. Hum Vaccin Immunother 2014;10(8):2147–216221.
[20] Pichichero ME, Casey JR, Almudevar A, Basha S, Surendran N, Kaur R, et al. Functional immune cell differences associated with low vaccine responses in infants. J Infect Dis 2016;213(12):2014–9.
[21] Pichichero ME, Deloria MA, Rennels MB, Anderson EL, Edwards KM, Decker MD, et al. A safety and immunogenicity comparison of 12 acellular pertussis vaccines and one whole-cell pertussis vaccine given as a fourth dose in 15-to 20-month-old children. Pediatrics 1997;100(5):772–88.
[22] Plotkin SA. Correlates of vaccine-induced immunity. Clin Infect Dis 2008;47 (3):401–9.
[23] Plotkin SA. Complex correlates of protection after vaccination. Clin Infect Dis 2013;56(10):1458–65.
[24] Shelly MA, Jacoby H, Riley GJ, Graves BT, Pichichero M, Treanor JJ. Comparison of pneumococcal polysaccharide and crm197-conjugated pneumococcal oligosaccharide vaccines in young and elderly adults. Infect Immun 1997;65 (1):242–7.
[25] Spijkerman J, Veenhoven RH, Wijmenga-Monsuur AJ, Elberse KE, van Gageldonk PG, Knol MJ, et al. Immunogenicity of 13-valent pneumococcal conjugate vaccine administered according to 4 different primary immunization schedules in infants: a randomized clinical trial. JAMA. 2013;310(9):930–7.
[26] Storsaeter J, Hallander HO, Gustafsson L, Olin P. Levels of anti-pertussis antibodies related to protection after household exposure to bordetella pertussis. Vaccine 1998;16(20):1907–16.
[27] Tashani M, Alfelali M, Barasheed O, Alqahtani AS, Heron L, Wong M, et al. Effect of tdap when administered before, with or after the 13-valent pneumococcal conjugate vaccine (coadministered with the quadrivalent meningococcal conjugate vaccine) in adults: a randomised controlled trial. Vaccine 2016;34 (48):5929–37.
[28] World Health Organization. Pneumococcal Vaccines: WHO Position Paper – 2012. Wkly Epidemiol Rec 2012;87(14):129–44.